A STUDY OF COUPLED INFLUENCE OF EVAPORATION AND FLUID FLOW INSIDE A WELD POOL ON WELDED SEAM FORMATION IN GMAW

O. MOKROV*, O. LISNYI*, M. SIMON*,
A. SCHIEBAHN* and U. REISGEN*

**RWTH Aachen University, ISF – Welding and Joining Institute, 52062, Aachen, Germany, lisnyi@isf.rwth-aachen.de*

DOI 10.3217/978-3-85125-615-4-06

ABSTRACT

Simulation of the gas metal arc welding (GMAW) process in the welding pool and welded plates requires to define such distributed parameters of the welding arc as heat, mass and electric current fluxes as well as arc pressure and drag forces on the free surface of the welding pool. Comprehensive approaches to define these parameters require to use three dimensional magneto-hydrodynamic arc plasma models. The high complexity of these models does not allow to use them widely for calculation. Nevertheless the most amount of available works use a simplified definition of arc source parameters as a predefined shape (e.g. circular or double ellipsoid law due to the Gauss distribution), that does not change during the calculation. In this work, a new approach is proposed to define the distributions of arc parameters not in the usual predefined shape, but in distributions, that are modified according to the calculated temperature of the free surface of the welding pool on which the arc heating, evaporation of the welding metal and hydrodynamics of the welding pool have their own coupled impact. The discussed approach was used in developing a mathematical model of GMAW process that can provide a numerical analysis of thermal, electromagnetic and hydrodynamic processes in the weld pool and welded plates. The model was used to study the proposed approach of arc parameters redistribution on the welded seam formation.

Keywords: arc welding, numerical simulation, cathode area, heat flux distribution, welded seam formation.

INTRODUCTION

The gas metal arc welding (GMAW) process is widely used in industries for manufacturing of metal constructions. The quality of a welded joint depends on a set of welding process variables that define conditions of the welding arc burning, the transfer mode of electrode droplets, the shape of the melted zone, the geometry of the welded seam, the chemical composition and heterogeneity, thermal cycles, that define the microstructure and the mechanical properties of the welded metal. A rational choice of welding process variables

requires investigations of physical processes taking place in the weld pool and welded plates. Limitations of experimental research methods caused the need to use mathematical modelling.

One of the main goals of the arc welding process modelling is the prediction of the temperature field, the weld seam geometry and the shape of the weld pool in dependence of the welding process variables. A solution of this task requires to develop appropriate physics-based models for the GMAW process. Calculation of physical processes in the welding pool and welding plates requires to define some parameters of the welding arc such as pressure, drag forces, heat, mass and electric current fluxes on the free surface of the welding pool.

The most comprehensive approach to define these parameters requires to use three dimensional MHD arc plasma models which consider evaporating anode (A) and cathode (C) areas. The high complexity of these models does not allow to use them widely for calculation. Nevertheless, most of the available works use a simplified definition of arc source parameters with usually circular shaped distribution [1, 2].

In this work, a new approach is proposed to define the distributions of heat flux, current density and arc pressure within the cathode area on the free surface of the welding pool. It was proposed to define them not in the usual circular shape, but in a distribution, that is modified according to the calculated temperature of the free surface of the welding pool on which the hydrodynamics of a welding pool and evaporation of welding metal have their own impact.

The intention of the present work is to use the discussed approach to develop a mathematical model of GMAW process that can provide a numerical analysis of thermal, electromagnetic and hydrodynamic processes in the weld pool and welding plates and estimate their influence on the weld seam formation.

DESCRIPTION OF A MATHEMATICAL MODEL

The model of the GMAW process considers physical phenomena of heat transfer, electromagnetics, hydrodynamics and deformation of weld pool free surface.

In order to simplify the mathematical model formulation, the following assumptions were made: fluctuations of the welding arc burning due to the electrode melting and droplet detachment are neglected; the hydrodynamics flow is Newtonian, uncompressible and laminar, the Boussinesq buoyancy approximation is applied; the droplets' frequency, initial velocity, temperature and diameter in dependence on welding parameters are calculated by given empirical equations. To speed up the calculation of weld pool hydrodynamics, ideas that were proposed in [3-4] were used. It is supposed, that the incoming droplet in the weld pool is considered as a non-mixed particle that keeps its mass and size. The trajectory of the droplet in the weld pool is determined numerically by integrating the equation of motion. The interaction between the droplet and liquid metal of the weld pool is determined by the droplet's trajectory due to viscosity and heat conductivity of liquid metal. When the velocity of the droplet becomes the same as the melt flow velocity it is considered that the droplet is accepted by the weld pool volume.

The calculation area includes the welding plates, the welding pool and the solidified metal of welded seam. The Cartesian stationary coordinate system (x, y, z) is used in the

calculation. The welding arc moves along x axis and gravity force is directed downward in z direction (Figure 1).

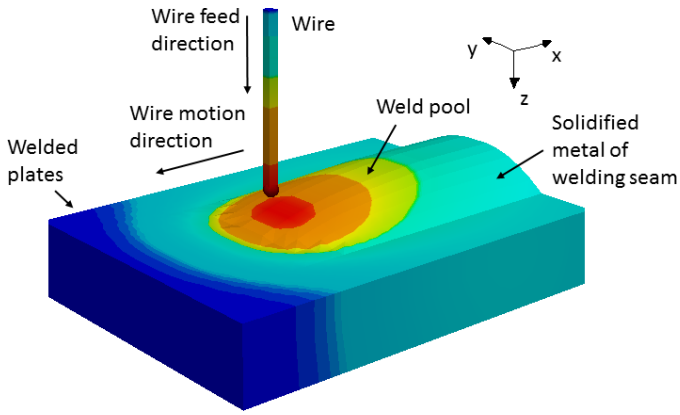

Fig. 1 Schematic representation of GMAW process.

Based on the above assumptions, the governing equations used to describe the GMAW process are given as follows: they include heat transfer (1), momentum transfer (2) and mass conservation (3), electrical current continuity (4), Maxwell's equations (5) and the deformation of weld pool free surface (6-7).

$$\frac{\partial h}{\partial t} + \nabla(\vec{u}h) = \nabla(\lambda \nabla \mathrm{T}) + \frac{\vec{j}^2}{\sigma} + S_{dh}\,; \tag{1}$$

$$\rho\left(\frac{\partial \vec{u}}{\partial t} + \nabla(\vec{u}\,\vec{u})\right) = -\nabla \mathrm{P} + \nabla(\mu \nabla \vec{u}) + \rho \vec{g} \beta_A T + \vec{j} \times \vec{B} + \overrightarrow{S_{du}}\,; \tag{2}$$

$$\nabla(\rho \vec{u}) = 0\,; \tag{3}$$

$$\nabla(\sigma \nabla \varphi) = 0\,; \tag{4}$$

$$\vec{\mathrm{B}} = \nabla \times \vec{\mathrm{A}},\ \nabla^2 \vec{\mathrm{A}} = \mu_0 \vec{\mathrm{j}}\,; \tag{5}$$

$$\upsilon \nabla(K^{-1} \nabla \xi) - \rho(\vec{g} \cdot \vec{n})(\xi - \xi_{max}) = P_{arc} + P_d;. \tag{6}$$

$$\int_{y_m}^{y_p} (\xi(\mathrm{x}_m, \mathrm{y}) - \xi_0) dy = \pi r_f^2 \frac{u_f}{u_w}; \tag{7}$$

where t is the time; $h = \int_{\mathrm{T}_0}^{T} c\rho\, dT + \chi\, \rho\, \eta$ is the enthalpy; c is the heat capacity; ρ is the mass density; T is the temperature; T_0 is the initial temperature; χ is the latent heat; η is the fraction of liquid metal ($\eta = 0, \mathrm{T} \le \mathrm{T}_S$; $\eta = 1, \mathrm{T} \ge \mathrm{T}_L$; $\eta = (\mathrm{T}\text{-}\mathrm{T}_S)/(\mathrm{T}_L - \mathrm{T}_S), \mathrm{T}_S < \mathrm{T} < \mathrm{T}_L$); T_L, T_S are the liquidus and solidus temperatures; u is the fluid flow velocity of liquid metal inside the weld pool; λ is the thermal conductivity; j is the electrical current density; σ is the electrical conductivity; P is the pressure; μ is the viscosity; g is the acceleration due to gravity; β_A is the thermal volumetric expansion coefficient of liquid metal; B is the magnetic induction; φ is the electrical potential (it is linked to the current

via Ohm's law $j = -\sigma\nabla\varphi$); A is the vector potential; μ_0 is the permeability of vacuum; ξ is the free surface position in z direction; υ is the surface tension; $K = \sqrt{1 + (\nabla\xi)^2}$ is the curvature of the free surface; $P_{arc} = \frac{3\mu_0 I^2}{4\pi}\frac{1}{\pi r_P^2}\, exp(-3(x_t^2 + y^2)/r_P^2)\, \beta(T, T_B)$ is the arc pressure; r_p is the arc pressure radius; $x_t = x_0 - u_w t$, x_0 is the current and beginning position of the welding arc; u_w is the welding velocity; β is the arc redistribution function; T_B is the boiling temperature; $P_d = \frac{3}{4}\pi r_d^3 \frac{3\rho u_d f_d}{\pi r_d^2} exp(-3(x_t^2 + y^2)/r_d^2)$ is the droplet impact pressure; u_d, f_d, r_d are the droplet velocity, frequency and radius.

The source terms considering the droplets' interaction with the weld pool are given as $S_{du} = \frac{1}{\delta V}\sum_{k=1}^{N} f_d A_k$, $S_{dh} = \frac{1}{\delta V}\sum_{k=1}^{N} q_d A_k$; where S_{du}, S_{dh} are the local values of mechanical momentum and heat sources due to the interaction between the droplets and the liquid metal of the weld pool; N is the instantaneous number of droplets that are present in a local volume δV; A_k is the surface area of a droplet; $f_d = (u_d - u)\mu/r_w$ is the mechanical interaction between the droplet and the liquid metal of the weld pool; u_d is the droplet velocity; r_w is the length of predefined boundary layer. The change of droplet kinematic momentum is tracking by expression $du_d/dt = f_d/\rho$. The heat flux between the droplet and the weld pool is given as $q_d = (T_d - T)\lambda/r_w$, T_d is the droplet temperature, T is the local temperature of liquid metal. The change of the droplet's heat content is given by $\partial h_d/\partial t = q_d\, A_k/\delta V$.

The deformation of the weld pool free surface is calculated using an equilibrium surface equation (6), considering the influence of surface tension, surface curvature, gravity, arc pressure and droplet impact pressure. ξ_{max} is determined by the integral equation of mass conservation (7) due to the assumption that the volume of metal fed from the wire is equal to the volume of weld reinforcement; y_p, y_m are the boundaries of molten metal in y direction, x_m is the boundaries of molten metal in x directions at the edge of solidification; ξ_0 is the initial coordinates of top surface before melting; r_f is the radius of electrode wire; u_f is the velocity of electrode wire feeding.

Boundary conditions for heat flux on the left (y=2Lg), right (y=-2Lg), front (x=0), back (x=8Lg) and bottom (z=Lg) surfaces were defined by eq. (8), where Lg is a space parameter. The heat flux on the top surface ($z = \xi$) was defined by eq. (9).

$$\lambda \frac{\partial T}{\partial n} = q_{NR} - q_{radi}; \tag{8}$$

$$\lambda \frac{\partial T}{\partial n} = q_{arc} - q_{NR} - q_{radi} - q_{evap}; \tag{9}$$

$$q_{NR} = \alpha(T - T_{out}); \tag{10}$$

$$q_{radi} = e\, \sigma_S\, (T^4 - T_{out}^4); \tag{11}$$

$$q_{arc} = \frac{\eta I U - W_d}{\pi r_h^2} exp\left(-3(x_t^2 + y^2)/r_h^2\right) \beta(T, T_B); \tag{12}$$

where n is the outward unit normal vector of the surface, α is the Newton-Richmann heat exchange coefficient, σ_S is the Stefan-Boltzmann constant, e is the surface emittance, T_{out} is the ambient temperature, q_{evap} is the evaporation heat flux, which is calculated by the evaporation model from [5], q_{arc} is the arc heating flux, η is the arc efficiency, I is the welding current, U is the drop of arc voltage, $W_d = c\rho\, \pi r_f^2\, u_f (T_d - T_{our})$ is the heat power consumed for heating of electrode wire and droplets, r_h - is the arc heating radius. The melt flow velocity along solidus temperature is set as $u = 0$. On the top surface the normal component of vector velocity is set as $u_n = 0$ and the tangential component of vector velocity τ is defined by surface thermo-capillary force $\frac{\partial u_\tau}{\partial n} = \beta_M \frac{\partial T}{\partial \tau}$; where $\beta_M = d\upsilon/dT$ is the temperature coefficient of surface tension. The electric potential at the bottom surface is set as $\varphi = 0$. At the top surface we adopt the following electric potential $\sigma \nabla\varphi = I/(\pi r_j^2)\, exp\left(-3(x_t^2 + y^2)/r_j^2\right)\beta(T, T_B)$ where r_j is the arc electrical radius. At other boundaries $\nabla\varphi = 0$. The gradient of the magnetic potential at all sides is set as $\nabla A = 0$. At the beginning of calculation $t=0$, $T=T_0$, $u=0$, $P=0$, $\varphi = 0$, $\xi = \xi_0 = 0$, $x_0 = 6L_g$. The calculation leads until $x_0 > 2L_g$.

CALCULATION METHODS

The mathematical model of the GMAW process was approximated by the finite volume method. A non-uniform rectangular spaced grid is used to describe the geometrical model approximation. A finer spacing grid (0.2 mm) was applied in melted area. The SIMPLER algorithm [6] is employed to calculate the fluid velocity fields. A restriction on the overheating of the weld pool free surface was considered due to the evaporation of the base metal. It was taken into account that the increase of evaporated mass flow leads to a decrease of the density of the electric current and heat generation in local areas of the cathodic layer. The used assumptions are aligned with the existing hypotheses of a preferential binding of the welding arc to the free surface of the welding pool. The initial distribution of arc parameters were defined by normal Gauss' law. During the calculation, a special iteration procedure was applied to obtain values of β function (it can be changed from 1 when $T < T_B$ up to 0 when $T >> T_B$). It limits the overheating of the welding pool surface above the boiling temperature. The values of r_P, r_H, r_j were recalculated according to changing β to keep the integral value of arc pressure, heating and electrical current as given constants).

The geometry of the weld pool was defined as D, B, G, L - the depth, width, height of reinforcement and length. The initial internal model parameters r_h, r_j, r_d, r_P were defined by experimental data due to providing less than 5% of numerical error for the weld pool geometry calculation, other parameters are given in Tables 1-2.

Table 1 Parameters of mathematical model

Property	Symbol, unit	Value
space parameter	L_g, *cm*	1.0
electrode radius	r_e, *cm*	$8.0 \cdot 10^{-2}$
arc voltage	U_0, *V*	32
welding velocity	u_w, *mm/min*	600
length of boundary layer	r_w, *cm*	$1.0 \cdot 10^{-2}$
velocity of electrode wire melting (I = 250-375 A)	u_f, *cm/s*	$-6.3 + 0.053 \cdot I$
arc efficiency	η	0.8
Stefan-Boltzmann constant	σ_S, *W cm^{-2} K^{-4}*	$5.67 \cdot 10^{-4}$
coefficient of radiation emission	χ *e*	0.4
coefficient of Newton-Richman heat exchange	α, *W cm^{-2} C*	$1.0 \cdot 10^{-3}$
magnetic permeability	μ_0, *g s^{-2}*	$1.26 \cdot 10^{-3}$
gravitational acceleration	*g, cm c^{-2}*	980.0
initial and ambient temperature	T_0, T_{out}, *C*	20.0
liquidus temperature	T_L, *C*	1514.0
solidus temperature	T_S, *C*	1443.0
boiling temperature	T_B, *C*	2860.0

Table 2 Parameters of mathematical model

Property	Symbol, unit	Value
latent heat of melting and solidification	χ, *J g^{-1}*	270.0
density of material	ρ, *g cm^{-3}*	7.6
coefficient of surface tension	υ, *g s^{-2-}*	$1.8\ 10^3$
heat capacity	*c, J g^{-1} C^{-1}*	0.5
thermal conductivity	λ, *W cm^{-1} C^{-1}*	0.45
electrical conductivity (T > 1000C)	σ, *om^{-1} cm^{-1}*	$1.0 \cdot 10^4$
cinematic viscosity	μ, *cm^2 s^{-1}*	$1.1 \cdot 10^{-2}$
coefficient of thermal volumetric expansion	β_A, *C^{-1}*	$1.4 \cdot 10^{-4}$
coefficient of thermal surface expansion	β_M, *C^{-1}*	$2.1 \cdot 10^{-3}$

EXPERIMENTAL PROCEDURE

The experiments were made for 100x100x10 mm plates of S235JR steel, 1.6 mm diameter welding wire of SG2 steel, electrode stick out 25 mm, direct current electrode positive (DCEP) power source supply. The experimental data of geometry of the weld bed was obtained. A digitized measurement of full 3-dimensional shape of weld bed was defined by a non-contact 3d laser profiling system, Figure 2. The welding parameters and sizes of the weld pool are given in Table 3.

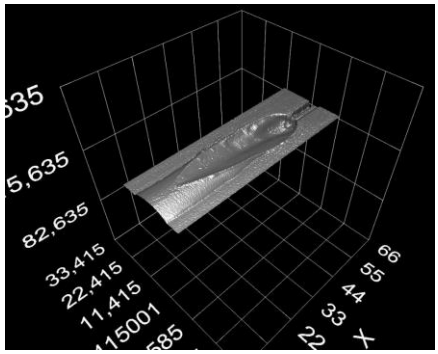

Fig. 2 3D scan of the weld bed .

Table 3 Experimental data of weld pool geometry

I,A	D, mm	B, mm	G, mm	L, mm
250	3.3	9.1	1.3	21.0
375	7.9	11.0	3.7	43.0

RESULTS AND DISCUSSION

Figure 3-4 shows the calculated results obtained due to the use of heat flux q_{arc} that is distributed by Gauss' law (GL).

Figure 3 shows the calculated results at 250 A. As the maximal temperature of the weld pool free surface 2840 C is lower than the boiling temperature of the welding material. The heat lost due to the evaporation is not significant and the effect of heat flux redistribution in the cathode area for this case does not appear. The velocity of electrode melting is 7 cm/s. The free surface of the liquid welding pool metal has no significant deformation as the arc pressure and droplet impact flow have no significant influence.

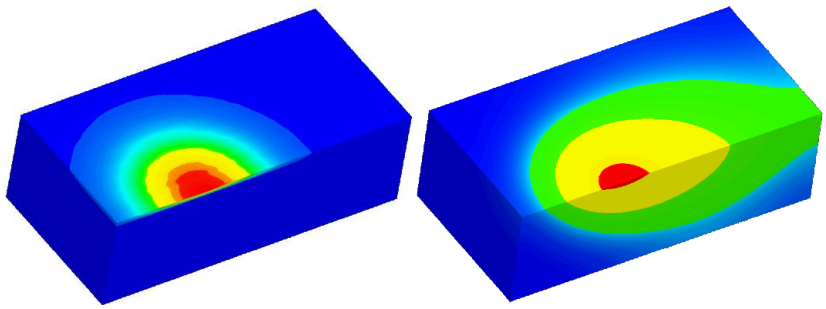

a b

Fig. 3 Heat flux (a) and temperature field (b) (I=250 A, v_{max} = 40 mm/s, q_{max} = $1.43 \cdot 10^5$ W/cm^2, T_{max} = 2840 C).

In this case the shape of the free surface is mostly defined by the surface tension force and the intensity of metal mass income due to the electrode melting rate. It indicates the surface mode of heat and mass transfer in the area of burning arc during GMAW process.

The convective flow of liquid metal inside the weld pool is formed mainly under the influence of thermo-gravitational and thermo-capillary forces. In this case the maximum velocity of liquid metal flow is 40 mm/s. The impact of the electromagnetic Lorentz force and forced convection due to the droplets income do not lead to a significant axial flow in the downward direction of the weld pool. In the central part of the weld pool, ascending liquid streams are formed. They transport the most overheated metal from the arc area along the free surface to the periphery of the weld pool. Near solidification borders, the convective streams of liquid metal change in the opposite direction and move along the bottom surface of the welding pool. Near solidification borders, the convective streams of liquid metal change in the opposite direction and move along the bottom surface of the welding pool.

Figure 4 shows the calculated results at the higher welding current 375 A. The velocity of electrode melting rate reaches 19 cm/s, the depression of weld pool free surface is 3.5 mm.

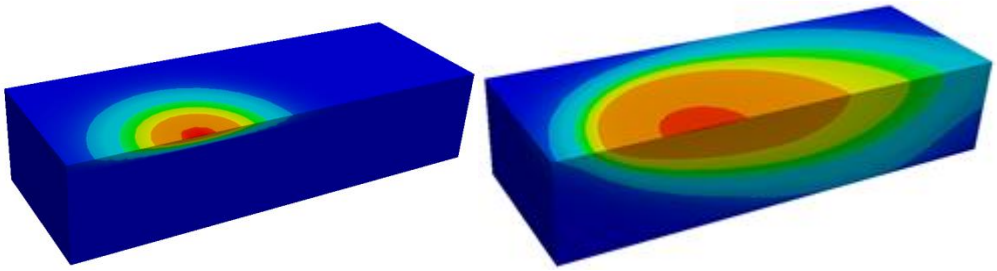

a b

Fig. 4 Heat flux (a) and temperature field (b) q_{arc} settled by Gauss' law (*I=375 A, v_{max} = 250 mm/s, q_{max} = 2.15·10^5 W/cm^2; T_{max} = 3150 C*).

The comparison between 250 A and 375 A shows a significant increase of the penetration depth, while the width of the melted zone becomes smaller (Table 3). This result is caused by the complex influence of two main factors that lead to the concentrated arc source impact on welding plates. The first factor is the significant deformation of the weld pool free surface due to the more intensive arc dynamic pressure and the droplet impact flow. It increases the temperature gradient and heat flux from the free surface of the weld pool to the melting front due to the decreasing of the thickness of liquid metal under the arc source. The second factor is the change of the liquid metal hydrodynamic flow pattern. In this case the convective flow inside the welding pool is formed mainly due to the electromagnetic Lorentz force and the forced convection due to the droplets mass income. Under the influence of these force factors the maximal velocity of convective flow reaches 200 mm/s. Inside the welding pool near the electrode tip a downward convective flow is formed. It transfers the most overheated metal from the arc area to the melting front. At the solid interface, the convective flow turns and goes along the bottom surface to the peripheral zones of the weld pool.

Figure 5 shows the calculated results obtained due to the use of heat flux q_{arc} that is redistributed due to the evaporated mass flow (EMF) at welding current 375 A. The maximal overheating above the boiling temperature in case GL is 290 C, in case EMF it is less than 35 C.

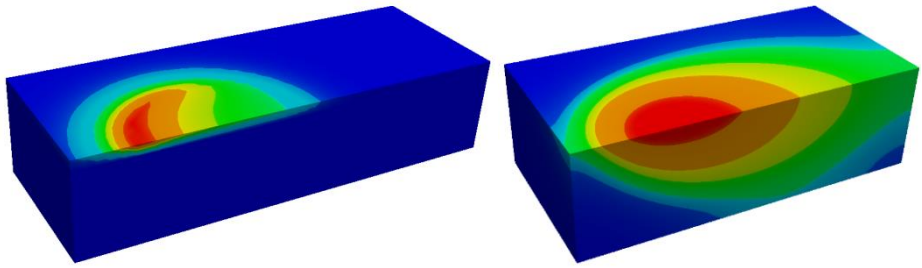

a b

Fig. 5 Heat flux (a) and temperature field (b) q_{arc} redistributed due to the evaporated mass flow, (*I=375 A, v_{max} = 200 mm/s, q_{max} = 1.5·10^5 W/cm^2; T_{max} = 2895 C*).

The higher overheating produces higher heat losses and as a subsequent result in the EMF case the depth of penetration incresed by 15%, the lengths of the weld pool is increased by 20% and the width of the weld pool is increased by 5%. Also, it has to be mentioned that in the EMF case the heat distribution has no axial symmetry and is stretched along the melting front of the weld pool. The highest density of the heat flux of the arc in the cathode area is shifted from the central region of the weld pool (under the electrode) towards the melting front of the weld pool. Due to this cause, the direction of heat and mass flow in the weld pool changes, which promotes an increase of the melting ability of the welding arc.

CONCLUSIONS

The developed mathematical model of GMAW process allows to investigate the formation of the temperature field in the welding plates, fluid flow inside the weld pool, geometry of the welding bed and welded seam in dependence on GMAW process variables.

The results of the calculations show that in case of redistributed heat flux q_{arc} with an increase of thermal power of the arc the highest density of the heat flux of the arc in the cathode area is shifted from the central region of the weld pool (under the electrode) towards the melting front of the weld pool. Due to this cause, the direction of heat and mass flow in the weld pool changes, which promotes an increase of the melting ability of the welding arc. With increasing depression of the free surface of the weld pool this effect amplifies.

The obtained calculations show that for a plate with a thickness of 10 mm, arc voltage 32 V, welding velocity 600 mm/min and at a current of 375 A, the effect of arc parameters redistribution leads to an increase in depth of penetration by 15%, in length of the weld pool by 20% and in width of the weld pool by less than 5%. The increase of melted metal volume in comparison with original Gauss' law distribution is caused by decreased heat losses due to evaporation. The calculation show that considering of arc bending can have influence on weld bed calculation.

The simulations show that with an increase of welding current the enthalpy transferred from the droplet to the weld pool has a stronger influence on the weld pool depth and the momentum transferred by the droplets has a stronger influence on the melt flow in the weld pool.

The developed model can be used as a base for the following investigation of the influences of the welding arc in GMAW process.

ACKNOWLEDGEMENTS

This work was carried out with the financial support of the Collaborative Research Centre SFB1120 (DFG (Deutsche Forschungsgemeinschaft) Sonderforschungsbereich) "Precision Melt Engineering" at RWTH Aachen University. For the sponsorship and the support we wish to express our sincere gratitude.

REFERENCES

[1] ZHEN NING CAO, PINGSHA DONG: *Modeling of GMA Weld Pools With Consideration of Droplet Impact*. J. Eng. Mater. Technol 120(4), 313-320 (Oct 01, 1998) (8 pages) doi:10.1115/1.2807020

[2] Z. YANG, T. DEBROY: *Modeling macro-and microstructures of Gas-Metal-Arc Welded HSLA-100 steel.* Metallurgical and Materials Transactions B, June 1999, Vol. 30, Issue 3, pp 483–493

[3] A.B. MURPHY: *A self-consistent three-dimensional model of the arc, electrode and weld pool in gas–metal arc welding*. J. Phys. D: Appl. Phys. 44, (2011), 194009 (11pp). doi:10.1088/0022-3727/44/19/194009

[4] A.B. MURPHY: *Influence of droplets in gas–metal arc welding: new modelling approach, and application to welding of aluminium*. Science and Technology of Welding and Joining, 2013 Vol. 18, No. 1, p.32-37.

[5] H.G. FAN, R. KOVACEVIC: *A unified model of transport phenomena in gas metal arc welding including electrode, arc plasma and molten pool*. J. Phys. D: Appl. Phys. 37 (2004) 2531–2544 PII: S0022-3727(04)77964-4

[6] M. CHOI, R. GREIF: *A study of the heat transfer during arc welding with applications to pure metals or alloys and low or high boiling temperature materials.* Numerical Heat Transfer, Vol. 11, 1987, pp. 477-489

[7] S.V. PANTANKAR: *Numerical Heat Transfer and Fluid Flow.* McGraw-Hill, 1980, New York